PROOF COPY 159306JVB

Fabrication of high Q square-lattice photonic crystal microcavities

K. Hennessy,[a] C. Reese, and A. Badolato
Department of Electrical and Computer Engineering, University of California, Santa Barbara, California 93106

C. F. Wang
Department of Physics, University of California, Santa Barbara, California 93106

A. Imamoğlu
Department of Electrical and Computer Engineering, and Department of Physics, University of California, Santa Barbara, California 93106

P. M. Petroff and E. Hu
Department of Electrical and Computer Engineering, and Department of Materials Science, University of California, Santa Barbara, California 93106

(Received 1 July 2003; accepted 6 October 2003)

This work discusses the fabrication of two-dimensional photonic crystal microcavities (PCMs) in a thin GaAs membrane. We have developed a fabrication process for square-lattice, single-hole-defect devices, a class of PCMs that is critically sensitive to fabrication accuracy, demonstrated coupling of InAs quantum dots to the cavity modes, and shown the sensitivity of the emission to the quality of the fabrication process. Reactive ion etching conditions were optimized to produce photonic crystal holes with smooth, straight sidewalls. To achieve uniform hole sizes throughout the device, we developed a method to correct the proximity effect introduced while defining the photonic crystal holes using electron-beam lithography. Resulting cavities have resonances with quality factors as high as 4000, which proves the quality of our fabrication. © *2003 American Vacuum Society.* [DOI: 10.1116/1.1629298]

I. INTRODUCTION

Two-dimensional photonic crystal microcavities (PCMs) formed in a thin semiconductor membrane are well suited for future nanoscale optoelectronic systems since they exhibit three-dimensional control of light while remaining compatible with planar nanofabrication techniques. In addition to classical communication applications, PCMs have attracted attention as possible laboratories to observe cavity quantum electrodynamic (CQED) phenomena. Techniques to suppress coupling to radiative modes have been used in PCM design to identify several PCMs based on a triangular lattice that are conducive to CQED experiments.[1–5] Cavities based on a square lattice have received relatively little attention since the photonic band gap in this geometry is comparatively small. Despite the reduced photonic gap, the existence of a high quality factor (Q) whispering-gallery-like mode (WGM) has been identified in a single-hole-defect PCM based on a square-lattice geometry (S1). The properties of this mode have been studied theoretically[6] and experimentally characterized at communication wavelengths.[7] Unlike many of the triangular-lattice PCMs designed for atomic experiments,[1–4] the antinode of the S1 WGM is located in the high-index region of the device, which is conducive to CQED with semiconductor quantum dots (QDs). We have previously shown high Q resonances in triangular-lattice PCMs internally excited by self-assembled InAs QDs.[8] Our current work aims to develop a fabrication process in the same material system for S1 PCMs, which are more critically dependent upon fabrication accuracy. Analyses of loss mechanisms in photonic crystal membranes suggest that fabrication accuracy is essential to achieve desired device performance.[9,10] Therefore, we prove the accuracy of our process by demonstrating high Q optical results.

II. DEVICE FABRICATION

The starting material is a heterostructure of (Al)GaAs embedded with five layers of self-assembled InAs QDs (2×10^{10} cm^{-2} QDs per layer) that constitute the active layer of our device with a spectral bandwidth from 870 to 970 nm. Simulations indicate the range of values of radius r and lattice constant a for photonic crystals supporting cavity modes in the QD emission spectrum. The photonic crystal pattern confines the light in the plane of the QD material and the formation of a membrane suspended in air provides strong vertical optical confinement. The membrane is chosen to be 180 nm, thick enough to fully confine the mode and thin enough to prevent the membrane from supporting higher-order modes. We have reported previously on the fabrication of membrane PCMs.[8] We have modified this process for square-lattice structures which are more critically dependent upon fabrication accuracy. A schematic of the process, incorporating these changes, is shown in Fig. 1. The photonic crystal pattern is defined in ZEP-520 A from Zeon Chemicals L.P. using a 50 kV JEOL JBX-5DII(U) electron-beam lithography (EBL) system and is then transferred into a SiN layer using CHF_3 reactive ion etching (RIE) to provide a more durable mask for the final pattern transfer into GaAs. Defining the photonic crystal holes by dry etching exhibits some

[a]Electronic mail: kjh@ece.ucsb.edu

PROOF COPY 159306JVB

PROOF COPY 159306JVB

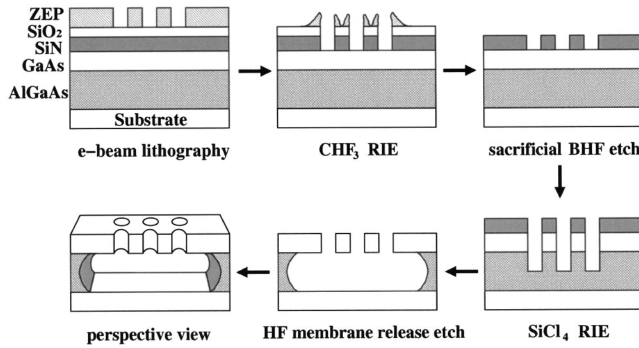

FIG. 1. Schematic of the fabrication process used to make photonic crystal membrane structures.

degree of inaccuracy and it has been shown that even slight sidewall inclination can result in substantial losses for guided modes.[9] Motivated to fabricate low-loss cavities, we have optimized the CHF_3 dry etching process to achieve optimal pattern transfer and straight sidewalls. More accurate pattern transfer occurs if the SiN is etched at very low CHF_3 pressure. The optimal CHF_3 etching conditions are: 3 sccm, 1 mTorr, and 250 V into 750 Å of nitride. The etch selectivity between ZEP-520A and SiN is degraded at this low pressure and compensated for by using a thick resist layer of 2500 Å. During this RIE step a significant amount of polymer is sputtered onto the SiN surface that inhibits subsequent pattern transfer into the GaAs layer. We use a SiO_2 sacrificial layer to correct this problem. A 200 Å film of PECVD SiO_2 is deposited between the SiN and ZEP-520 A layers. After EBL and the CHF_3 RIE step, the sputtered polymer is released from the SiN surface by immersing the sample in (5:1) $BHF:H_2O$ for 20 s. The selectivity between SiO_2 and SiN in this wet etch is 16:1, ensuring that negligible etching of the SiN occurs. The resulting clean SiN etch mask provides accurate pattern transfer into the GaAs device layer using $SiCl_4$ RIE. Immersion in a (5:1) $H_2O:HF$ solution undercut etches an $Al_{0.7}Ga_{0.3}As$ layer to form the freestanding membrane structure. The final photonic crystal holes are very circular, as shown in Fig. 2 (left) and have straight, smooth sidewalls as shown in Fig. 2 (right).

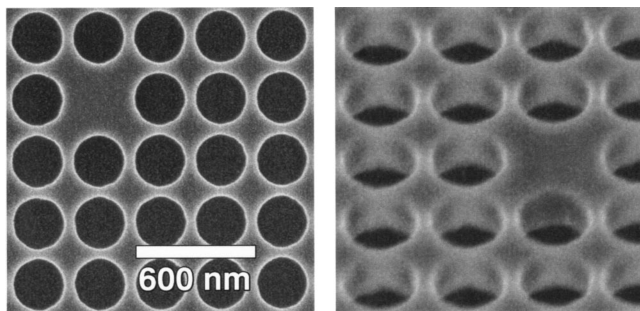

FIG. 2. Top view (left) and 45° (right) scanning electron micrographs of a single-defect photonic crystal microcavity with a 300 nm lattice constant and 180 nm membrane thickness.

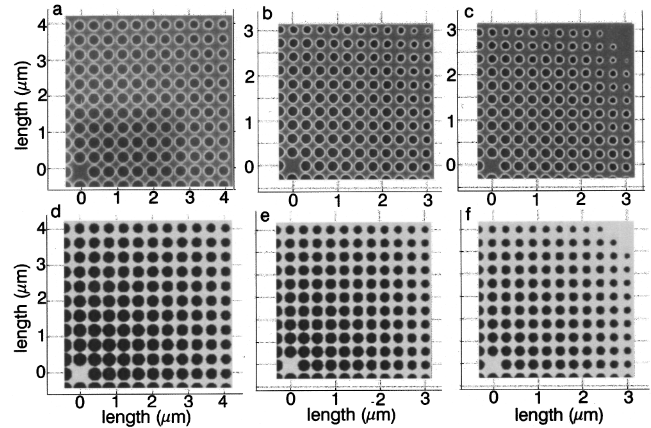

FIG. 3. Moderate variation of hole size in one quadrant of a square-lattice microcavity with a lattice constant a of 400 nm (a) agrees well with the predicted variation (d). More variation occurs in a smaller device ($a = 300$ nm) experimentally (b) and in simulation (e). Very strong variation is seen in an underexposed microcavity of lattice constant 300 nm (c) and agrees with simulations (f) predicting that the dose in the outermost holes does not clear the resist.

III. PROXIMITY EFFECT CORRECTION

Due to their square geometry, photonic crystals based on a square lattice and fabricated using EBL are susceptible to a variation in photonic crystal hole size over distances of many lattice periods. Our S1 PCMs are fabricated with ten lattice periods surrounding the defect and substantial variation in hole size can be seen in the last several periods in Fig. 3(b) where we have reproduced only the upper right quadrant of the device to allow closer inspection of the individual photonic crystal holes. The variation is attributed to inadvertent exposure in the resist due to the forward- and backscattering of electrons in the resist and substrate, respectively, often referred to as the proximity effect. Small variation in hole size in 2D photonic crystals should not substantially affect device performance, but it has been computed that substantial size fluctuation, such as shown in Fig. 3(b), will greatly reduce the size of the photonic gap.[10] As previously mentioned, the square lattice exhibits a relatively small band gap, making it especially critical that the proximity effect should be corrected. To perform this correction using computational methods, it is essential to first determine the point spread function (PSF) of the electron beam in this material system. This function characterizes all forward- and backscattering of electrons in the system and it has been shown that the PSF on GaAs can be approximated by the following equation:[11]

$$f(r)=\frac{1}{\pi(1+\eta+\nu)}\left(\frac{1}{\alpha^2}e^{-r^2/\alpha^2}+\frac{\eta}{\beta^2}e^{-r^2/\beta^2}+\frac{\nu}{2\gamma^2}e^{-r/\gamma}\right). \tag{1}$$

We determined the numerical values of the parameters in Eq. (1) by systematically varying each one and noting its effect on the final electron dose distribution in the resist layer. This distribution was calculated by convolving $f(r)$ with the electron beam profile function (assumed to be a Gaussian distribution of width 15 nm) and convolving the result with a

PROOF COPY 159306JVB

PROOF COPY 159306JVB

function representing a PCM that has a value of one in the photonic crystal holes and zero otherwise. By defining a clearing dose that results in photonic crystal holes of the intended size at the *center* of the device, we can see, for a given α, β, η, γ, and ν, how the hole size varies from the center to the edge of the device. The parameters in Eq. (1) were varied until predicted devices matched SEM micrographs of processed devices of varying *r, a*, and electron dose. Our computational predictions agree best with fabricated devices when the parameters are: α=0.035 μm, β=3.78 μm, γ=0.38 μm, η=0.75, and ν=0.54. Using this PSF, we predict hole size variation in S1 devices as shown in Fig. 3. In this figure, the images on the top row are SEM micrographs and the corresponding simulation results for the same device geometry and electron dose are shown in the bottom row. We predict modest variation of hole size for PCMs with large lattice constant (a=400 nm) as shown in Figs. 3(a) and 3(d) for experiment and simulation, respectively. Significant variation occurs in PCMs with smaller a =300 nm as shown in Figs. 3(b) and 3(e). The effects of under/over exposure were also modeled and, as an example, a device resulting from 5% less electron dose is shown in Figs. 3(c) and 3(f) for experiment and simulation, respectively. Since this PSF can be used to predict the final dose distribution of many PCMs of varying *a, r*, and electron dose, it must be representative of the forward/backscattering in our material system and can be used to correct the proximity effect.

Full proximity effect correction can involve a detailed, pattern-dependent, point-by-point dose correction. In our case, we had a simple, repetitive pattern where the major feature size change involved the photonic crystal holes at the periphery of the pattern. In order to achieve a fairly rapid, sufficiently simple compensation of dose to those peripheral holes, we adopted the method of writing extra features near the corner of the pattern. This elevates the electron dose there, increasing the size of the outermost holes. By using the method described above to calculate the total electron dose distribution in the resist, we simulated the effect of writing extra features around the corners of S1 PCMs. By varying the size, location, and electron dose of these extra features by trial-and-error, and then analyzing the resulting predicted devices, we designed a pattern that limits variation in hole size across the device to under a few percent. Optical measurements, presented in a later section, were used to establish that this was adequate correction to achieve desired device performance. The corrected pattern is shown in Fig. 4(a) for one quadrant of the device. The extra features are given a relatively high electron dose compared to the photonic crystal holes, up to 12 times as much in certain areas. Since the device is a suspended membrane, we designed the extra features so that they did not completely surround the PCM. Such a pattern would cause the device to collapse. The calculated electron dose distribution for the corrected devices is shown in Fig. 4(b) and, at a specific clearing dose, produces the device shown in Fig. 4(d). Real devices were fabricated with the extra corner features predicted by our simulations. A corrected device is shown in Fig. 4(c) and it is apparent that the extra features around the PCM produce holes with negligible variation in size while preserving the mechanical integrity of the membrane. The size variation is quantified in the inset of Fig. 5 where r/a is plotted as a function of lattice period along the diagonal for two devices with a=300 nm, one without correction and one incorporating the extra features. The range of application of this form of proximity correction includes all S1 PCMs resonant in our QD emission range (a from 290 to 310 nm). We do not report on its applicability for patterns outside this regime.

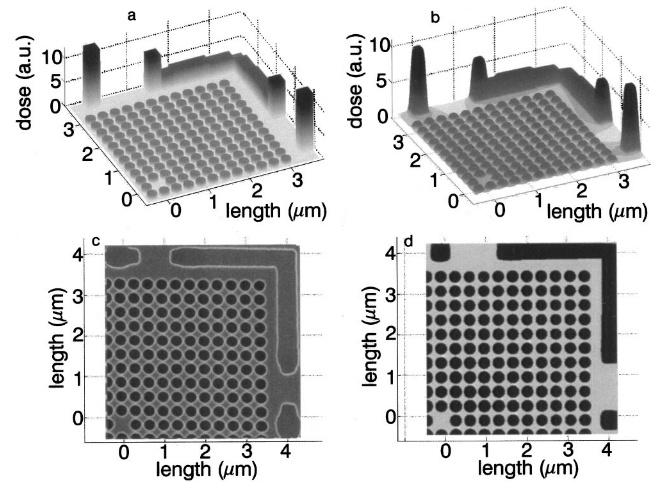

FIG. 4. One quadrant of the optimal pattern to write using electron-beam lithography to produce a photonic crystal with negligible variation in hole size (a) and the resulting calculated electron dose distribution in the resist (b). A device fabricated from this pattern (c) agrees well with simulations (d).

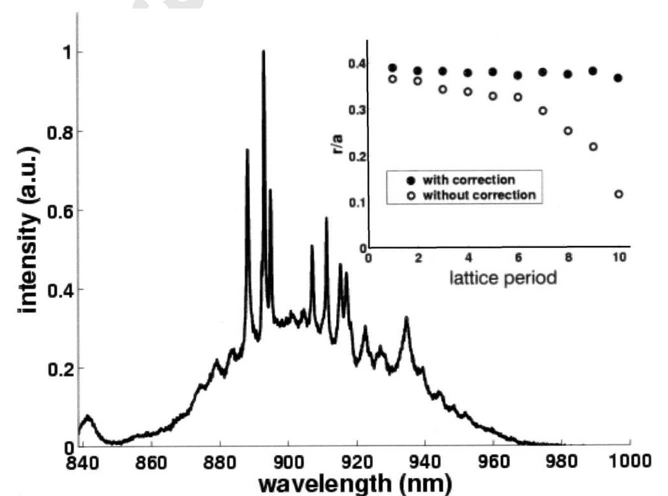

FIG. 5. Photoluminescence from a square-lattice microcavity with substantial variation in hole size due to uncorrected proximity effect from the electron beam lithography. The inset quantifies the hole size variation in terms of radius r divided by lattice constant a as a function of lattice position along the diagonal and is compared to a device incorporating proximity effect correction.

PROOF COPY 159306JVB

PROOF COPY 159306JVB

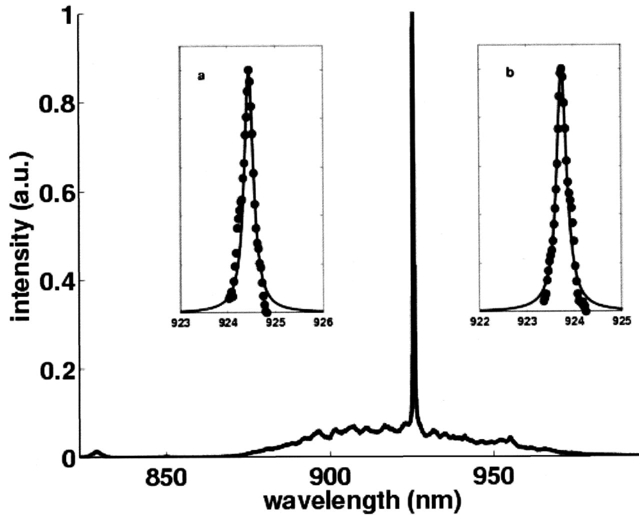

FIG. 6. Photoluminescence (PL) from a typical single-defect, square-lattice microcavity of lattice constant $a = 300$ nm and $r/a = 0.37$. The variation in hole size throughout this device is negligible. High-resolution PL is displayed in the insets for a slightly different geometry ($a = 300$ nm and $r/a = 0.38$), showing the high Q values of (a) 4000 and (b) 3600 in two separate, but nominally identical, devices.

IV. OPTICAL CHARACTERIZATION

Spatially resolved photoluminescence (PL) measurements were performed on S1 cavities of varying a and r using an external-cavity diode laser operating at 780 nm and exciting the sample surface with 130 μW of power in an estimated 3 μm spot size. The samples were mounted in a He-flow cryostat and cooled to 4 K. Further details of the experimental method have been described previously.[12] The self-assembled InAs QDs produce a continuous emission spectrum from 870 to 970 nm due to size variations. Using the QDs to decorate the cavity modes, we observed a difference in the spectra from devices with significant variation in hole size (uncorrected proximity effect) and devices where the variation in r/a was less than a few percent across the device. A spectrum from an uncorrected device is shown in Fig. 5, where the many, closely spaced resonances correspond to defect modes resulting from aperiodic hole r. In contrast, single-mode spectra is taken from devices with uniform hole r, as shown in Fig. 6, when a is between 290 and 310 nm. The spectrum in Fig. 6 corresponds to a PCM of $a = 300$ nm and $r/a = 0.37$. Cavities with lattice constants outside the range 290–310 nm were resonant outside of the QD emission spectrum. We measured the Q factor of these modes by collecting PL with a monochromator having a spectral resolution of 0.05 nm and fitting the spectra to Lorentzian functions. Cavities with $a = 300$ nm, $r/a = 0.38$, and $t/a = 0.6$ (where $t = 180$ nm is the thickness of the GaAs membrane) were of the highest quality and high-resolution spectra from two separate, but nominally identical, devices are shown in of Figs. 6(a) and 6(b) fit to Lorentzians of $Q = 4000$ and 3600, respectively.

V. CONCLUSION

We have optimized a fabrication process for defining photonic crystals in a thin GaAs membrane. By using very low pressure RIE to define the SiN etch mask and removing sputtered polymer from the surface of the mask prior to pattern transfer into the GaAs, we have achieved circular photonic crystal holes with smooth, straight sidewalls. We have proposed a simple technique for correcting hole size fluctuations resulting from the proximity effect. This correction is critical in the fabrication of square-lattice PCMs due to their relatively small photonic band gap and geometry that is susceptible to errors produced by the proximity effect. To test our fabrication process, S1 PCMs of varying a and r/a, exhibiting negligible hole size variation, were optically characterized and shown to support high quality resonances with Q as high as 4000. The observation of emission within the narrow bandwidth defined by the S1 band gap into high Q modes is only possible with much attention paid to the accuracy of the device fabrication. We have achieved this with the fabrication process reported in this article.

ACKNOWLEDGMENTS

The authors thank William Mitchell for assistance with the electron-beam lithography system, Dennis Prather for valuable FDTD simulations of these devices, the IGERT Program of the National Science Foundation for support under Award No. DGE-9987618, and DARPA for Grants QUIST MDA 972-01-1-0027 and CNID DMEA 90-02-2-0215.

[1]J. Vučković, M. Lončar, H. Mabuchi, and A. Scherer, Phys. Rev. E **65**, 016608 (2001).
[2]T. Yoshie, J. Vučković, and A. Scherer, Appl. Phys. Lett. **79**, 4289 (2001).
[3]J. M. Geremia, J. Williams, and H. Mabuchi, Phys. Rev. E **66**, 066606 (2002).
[4]J. Vučković, M. Lončar, H. Mabuchi, and A. Scherer, IEEE J. Quantum Electron. **38**, 850 (2002).
[5]J. Vučković and Y. Yamamoto, Appl. Phys. Lett. **82**, 2374 (2003).
[6]H.-Y. Ryu, J.-K. Hwang, and Y.-H. Lee, IEEE J. Quantum Electron. **39**, 314 (2003).
[7]H.-Y. Ryu, S.-H. Kim, H.-G. Park, and Y.-H. Lee, J. Appl. Phys. **93**, 831 (2003).
[8]C. Reese, B. Gayral, B. D. Gerardot, A. Imamoğlu, P. M. Petroff, and E. Hu, J. Vac. Sci. Technol. B **19**, 2749 (2001).
[9]Y. Tanaka, T. Asano, Y. Akahane, B.-S. Song, and S. Noda, Appl. Phys. Lett. **82**, 1661 (2003).
[10]H.-Y. Ryu, J.-K. Hwang, and Y.-H. Lee, Phys. Rev. B **59**, 5463 (1999).
[11]S. A. Rishton and D. P. Kern, J. Vac. Sci. Technol. B **5**, 135 (1987).
[12]C. Reese, C. Becher, B. D. Gerardot, P. M. Petroff, A. Imamoğlu, and E. Hu, Appl. Phys. Lett. **78**, 2279 (2001).

PROOF COPY 159306JVB

PROOF COPY 159306JVB